Jaroslaw LUSZCZ

Gdansk University of Technology

Motor Cable Effect on the Converter-Fed AC Motor Common Mode Current

Abstract. *Investigation of conducted EMI generation in AC motor drives fed by pulse width modulated voltage converters requires to consider parasitic capacitances in converters, motor windings and feeding cables to be taken into account. Motor voltage transients and related common mode currents are significantly correlated with resonance effects occurring in load circuits. The levels of intensity of these phenomena depend noticeably on frequency dependent impedance characteristic of converter load. An analysis of frequency converter load impedance characteristics allows for identification of frequency ranges in which the foremost contributions to EMI noise generation have voltage ringing phenomena associated with load parasitic capacitances. This paper presents a method to model an AC motor with a feeding cable in conducted EMI frequency range up to 30 Mhz. Distributed parasitic capacitances of AC motor windings are modeled as a ladder circuit. The developed circuit model allows for an analysis of the influence of the motor feeding cable parameters on common mode currents generated in AC motor drive system, particularly in AC motor itself. The simulation results obtained based on the proposed model are verified by the experimental tests which were carried out for an exemplary adjustable speed AC motor drive application.*

Streszczenie. *Analiza zaburzeń elektromagnetycznych przewodzonych w przekształtnikowych układach napędowych wymaga uwzględniania pojemnoci pasożytniczych wystepjących w przekształniku, uzwojeniach silnika oraz kablu zasilającym silnik. Dynamiczne zmiany napięć na uzwojeniach silników zasilanych z przekształtników częstotliwoci PWM oraz związane bezporednio z nimi składowe wspólne prądów zaburzeń przewodzonych są istotnie związane z zjawiskami rezonansowymi zachodzącymi w obciażeniu przekształnika. Intensywność występowania tych zjawisk jest zalezna od charakterystyki czestotliwociowej impedancji obciązenia, czyli uzwojeń silnika asynchonicznego wraz z kablem zasilającym. Analiza charakterystyki czestotliwociowej impedancji obciążenia pozwala na identyfikację zakresów czestotliwoci w których znaczacy wpływ na emisję zaburzeń przewodzonych mają zjawiska rezonansowe związane z pojemnociami pasożytniczymi w obwodzie obciązenia przekształnika. W referacie zprezentowano metodę szeropopasmowego modelowania uzwojeń silnka wraz z kablem zasilającym w zakresie częstotliwoci zaburzeń przeowdzonych do 30 MHz. Pojemnnści pasozytniczne cząstkowe uzwojeń silnika zostały zamodelowane poprzez pojemnoci zastepcze o strukturze drabinkowej. Zaproponowany model obwodowy pozwala na badanie wpływu parametrów kabla zasilajacego silnik na poziomy generowanych prądów zaburzeń wspólnych generowanych w przekształtnikowym układzie napędowym, a w szczególności w silniku. Wyniki uzyskane z przeprowadzonych badań symulacyjnych z wykorzystaniem opracowanego szerokopasmowego modelu obwodowego zostały zweryfikowane eksperymentalnie dla wybranych układów przekształtnikowych.* ***(Wpływ kabla silnikowego na prądy zaburzeń wspólnych generowane w przekształtnikowych układach napędowych z silnikami asynchronicznymi)***

Keywords: adjustable speed drives, ASD, conducted EMI, electromagnetic compatibility, EMC, common mode currents
Słowa kluczowe: przekształtnikowe układy napedowe, zaburzenia elektromagnetyczne przewodzone, kompatybilność elektromagnetyczna, EMC, składowe wspólne prądów zaburzeń

Introduction

Frequency converters commonly applied in contemporary adjustable speed drives (ASD) are a cause of accompanying undesirable high-frequency (HF) side effects in the powered AC motor and supplying grid [1]-[6]. Increase of pulse width modulation carrier frequency and decrease of converter transistors' switching time intensify existing HF problems in various ways. One of the foremost problems related to these phenomena is generation of high frequency stray current pulses flowing through drive components due to high levels of output voltage steepness (*dV/dt*) and unavoidable parasitic capacitances [7]-[9].

High frequency stray currents, flowing in conducting components of the ASD due to the existence of parasitic inter-capacitances, are not limited by standard regulations related to EMC of power electronic converters. Nevertheless, the foremost consequence of the stray HF current flow, especially through the parasitic capacitances, is the generation of HF voltage components spreading into all conductive elements of the ASD system. These HF voltage components, especially common mode (CM) voltages, are highly hazardous and are the fundamental origin of conducted EMI emission of power electronic converters. Detailed modeling of an ASD system in a wide frequency range for analyzing all interactions between a PWM voltage converter and an AC motor with cable is challenging and requires use of complex methods and broadband models [10]-[13].

The most difficult problem to model inverter fed AC motor drives in a wide frequency range is accurate identification of parasitic parameters of all drive components, especially in HF range. In the conducted EMI frequency range, usually up to *30 MHz*, the predominant model identification problem is related to parasitic capacitances of system components. These capacitances induce various HF objectionable effects such as: local resonances in parasitic sub-circuits and increased flow of harmful CM currents affiliated to them [3], [5], [14]–[20].

Increased CM currents generated on the output side of the frequency converter due to the extraordinary resonance effects in the feeding cable and the AC motor windings propagate to all the surrounding circuits and return back to the supply grid through the frequency converter. This paper presents a method for analyzing the influence of motor feeding cable on the motor CM currents flowing through parasitic capacitances between motor windings, stator and rotor. The proposed identification method of the load broadband circuit model parameters is based on the load impedance frequency characteristics analysis [9]. Determination of the most meaningful resonance frequencies observed on the load impedance characteristic allows for a ladder circuit model configuration arrangement with the appropriate number of rungs. Using this method the reasonable complexity level of the model can be maintained, what is essential for its parameter identification difficulty level.

Generation of Common Mode Currents in ASD

Analysis of CM currents propagation in the ASD is mostly related to the load side of frequency converter, which is usually voltage source pulse width modulated (PWM) controlled inverter with IGBT switches. In a such type of inverter, the output voltage steepness (*dV/dt*) is usually high because the bipolar DC bus voltage commutation during transistor switching time and additional switching transients. Nevertheless, contemporary line side PWM controlled rectifiers can also have significant effect on the CM currents generation but only the ASD with a line side diode rectifier has been analyzed in the presented investigation. This simplification allows recognizing more clearly motor cable effects on the

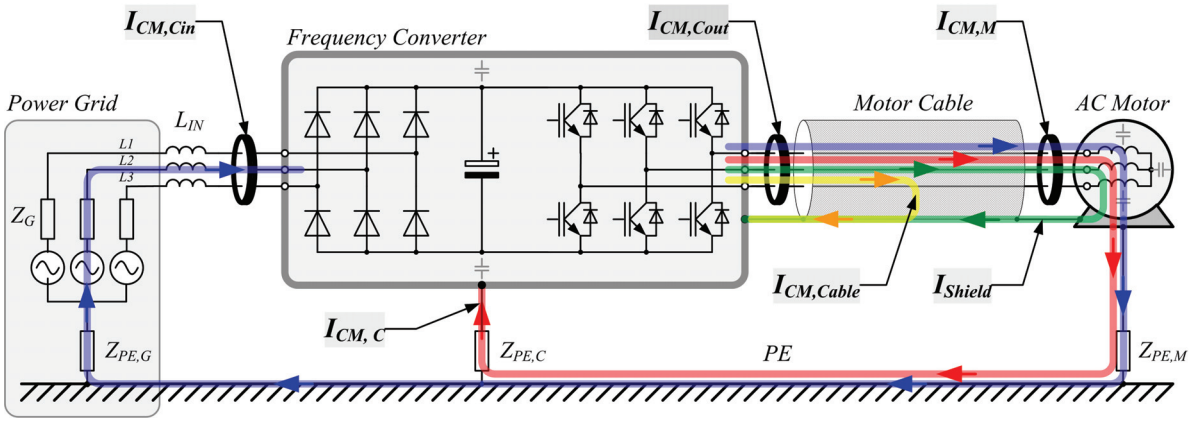

Fig. 1. The most significant common currents loops existing in a typical ASD with shielded motor cable

evaluated phenomena by minimizing simultaneous influence of line side converter. In a typical ASD configuration with AC motor fed by shielded cable presented in Fig. 1 four meaningful CM current loops can be emphasized:

- the first one $I_{CM,Cable}$ which is relatively the small loop and allow for CM current flow between energized motor cable wires and cable shield connected to output side of the converter due to cable internal capacitances,
- the second one I_{Shield} which carry most of motor CM current flowing through winding capacitances back to grounded converter chassis through motor cable shield grounded on both ends by converter and motor stator
- the third one $I_{CM,C}$ which carry the part of motor CM current flowing through ground connection between converter and motor other than motor cable shield, usually it is protective earth installation PE characterized by equivalent impedance of motor grounding connection $Z_{PE,M}$ and converter grounding connection $Z_{PE,C}$.
- the fourth one $I_{CM,Cin}$ which is the largest loop and conducts the remain part of motor CM current by the electric power grid impedance Z_G and power grid grounding impedance $Z_{PE,G}$.

CM currents loops presented in Fig. 1 show that motor feeding cable and its parameters are essential for CM currents generation and sharing between motor windings and feeding cable. According to presented in Fig. 1 circuit diagram the total CM current of converter is a sum of CM currents of motor windings and feeding cable (1). Nevertheless, the distributed character of parasitic capacitances cause many resonance interactions between a motor winding and a feeding cable, which complicate the analysis of CM currents distribution.

$$I_{CM,Cout} = I_{CM,M} + I_{CM,Cable} \tag{1}$$

Analysis of the CM currents in ASD is problematic because of difficulty to identify impedance-frequency characteristics of some parts of the CM current circuit, especially the power grid impedance, converter to ground impedance and the converter load impedance within the analyzed frequency range. Difficulties with determination of inverters load CM impedance are associated with parasitic capacitances of the motor windings and the feeding cable with reference to the ground. The parasitic capacitances are essential for the converters' load CM impedance changes. Distributed character of the parasitic capacitances in combination with rapid voltage changes induces transmission line reflection effects in the motor feeding cable and motor windings. The impedance mismatch between the inverter outputs, the feeding cable and the motor windings usually exist and complicates the analysis.

Broadband Modeling of AC Motor Windings

Broadband modeling of AC motor windings with a feeding cable is complicated because of distributed parasitic capacitances which should be determined. Complex and irregular distribution of these parasitic capacitances along the motor windings make identification process particularly difficult. The effortlessness of the identification of the parameters of the AC motor windings model is the main motivation for developing rationally simplified models.

A simplified model of distributed capacitances in AC motor windings in a wide frequency range can be formulated based on a ladder circuit model with an appropriate number of rungs - adequate for the given frequency range and expected accuracy. This simplification can be effectively used in a frequency range in which lumped circuit models are not accurate enough and detailed determination of distributed parasitic parameters of the evaluated system is too complicated. General configuration of the proposed circuit model with the N – step ladder circuit is presented in Fig. 2.

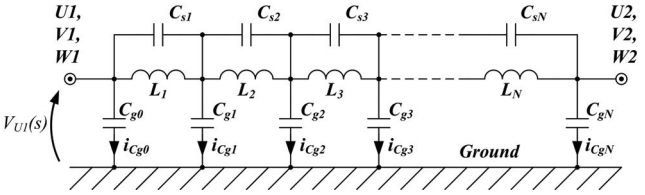

Fig. 2. Distributed parasitic capacitances between motor's windings and grounded stator, simplified lumped representation by N-step LC ladder circuit

The CM impedance of motor windings $Z_{M(CM)}$ as a relation between winding terminals voltage *U1, V1, W1* and the total CM current I_{CM} flowing through the distributed winding to the ground capacitances C_{gk} can be formulated based on the proposed circuit model as follows (**??**).

$$Z_{M(CM)}(s) = \frac{V_{U1}(s)}{\sum_{k=0}^{N} i_{Cgk}(s)} \tag{2}$$

Assuming that the winding self capacitances C_{s1}, C_{s2} , ..., C_{sN} are usually considerably smaller than the winding-to-ground capacitances C_{g0}, C_{g1} ,..., C_{gN}, the evaluated transfer impedance can be determined analytically

based on the presented circuit model using formula (3).

(3)
$$Z_{M(CM)}(s) \approx \cfrac{1}{sC_{g0} + \cfrac{1}{sL_1 + \cfrac{1}{sC_{g1} + \ldots + \cfrac{1}{sL_N + sC_{gN}}}}}$$

The reflection coefficient characteristic $\Gamma(s)$ at motor windings terminals for a given source impedance Z_0=50 Ω can be determined using formula (4). An example of the simulated reflection-frequency characteristic of the evaluated AC motor is presented in Fig. 3.

(4)
$$\Gamma(s) = \frac{Z_{T(CM)}(s) - Z_0}{Z_{T(CM)}(s) + Z_0}$$

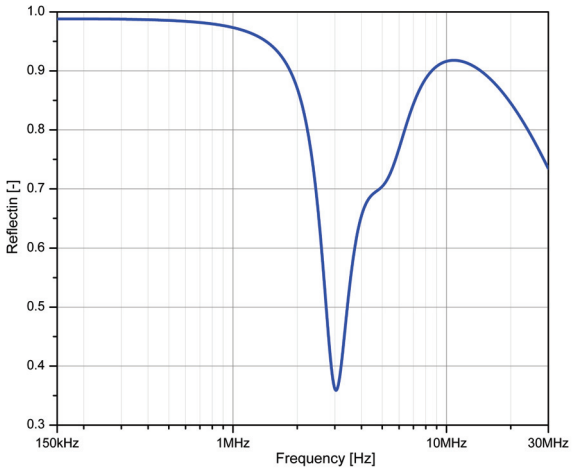

Fig. 3. Reflection characteristic of the evaluated AC motor at winding terminals

Modeling of an AC Motor Feeding Cable

Shielded power cables, commonly used in converter fed AC motor drives, can be represented as three conductor lines referenced to the ground. The cable shield represents the reference ground and equalizes conductors to ground parasitic capacitances, thus for broadband modeling the symmetrical circuit model of lossy transmission line can be implemented (Fig. 4).

Impedance related parameters of the AC motor feeding cable and its length are essential for the ASD general performance and cable influence on the conducted and radiated EMI emissions. Commonly used lengths of AC motor cables are from few meters up to few hundreds of meters long and are divided into two classes: short and long cables. A critical cable length is defined for various typical ASD applications which usually means that for the feeding cable longer than the critical length adverse effects are expected to appear intensively and some protective methods should be applied. The critical length depends on spectral characteristics of transmitted signals and pulse propagation velocity. Therefore, the critical cable length can be referenced to the shortest wavelength of transmitted signals.

Theoretically, a critical cable length, which allows to estimate exposure of the ASD to reflection phenomena in the AC motor cable, is commonly calculated based on the converter output voltage rise time t_r. The wavelength related to the voltage rise time can be calculated using formula (5) where ν

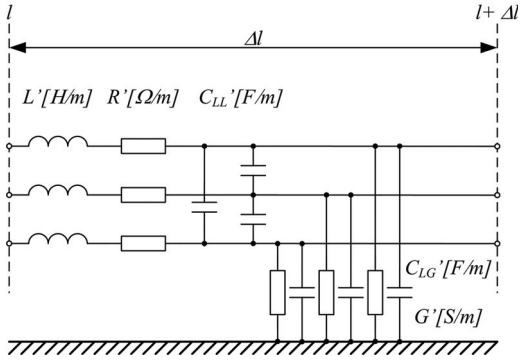

Fig. 4. Classic lossy transmission line circuit model of three conductor shielded power cable characterized by per unit parameters: resistance *R'*[Ω/m], inductance *L'*[H/m], capacitances C'_{LL}, C'_{LG} [F/m] and conductance *G'*[S/m]

is signal propagation velocity in the evaluated cable.

(5)
$$\lambda = t_r \cdot \nu$$

The signal propagation velocity in typical power cables is related to the relative dielectric permeability of cable insulation ϵ_r (6) and also correlated with propagation factor k_p, which can be determined based on the "per meter" parameters of cable according to formula (7) where inductance L_0 and capacitance C_0 are equivalent per unit length parameters [21].

(6)
$$\nu = \frac{1}{\sqrt{L_0 C_0}} = \frac{1}{\sqrt{\mu_0 \varepsilon_0}} \cdot \frac{1}{\sqrt{\varepsilon_r}} = \frac{1}{c_0} \cdot \frac{1}{\sqrt{\varepsilon_r}}$$

(7)
$$k_p(s) = \sqrt{(R_0 + sL_0)(G_0 + sC_0)}$$

Generally, the signal propagation velocity in power cables is approximately two times smaller than the light speed c_0, for the reason that dielectric permeability for typical cables insulations varies from 3 to 8, so obtained velocity is usually within the range of 40-60 % of the light speed. The characteristic impedance of cable $Z_C(s)$ (8) allows determining the reflection coefficient Γ at the motor terminals using (9) where $Z_{M(CM)}(s)$ is the motor windings input impedance.

(8)
$$Z_C(s) = \sqrt{\frac{R_0 + sL_0}{G_0 + sC_0}} \approx \sqrt{\frac{L_0}{C_0}}$$

(9)
$$\Gamma(s) = \frac{Z_{M(CM)}(s) - Z_c(s)}{Z_{M(CM)}(s) + Z_c(s)}$$

For the given frequency of transmitted signal, the critical cable length can be correlated to the wavelength determined by consideration of the real velocity of the signal propagation. The minimum length of the cable for which the reflection effects can be significantly increased is $\lambda/4$. Parameters per length of presented type of transmission line model for particular power cable can be determined by measuring the cable CM impedances in open circuit and short circuit configurations of far end [3].

Feeding Cable Impact on the Motor CM Currents

High frequency interactions between an AC motor and a feeding cable can be analyzed by simulation using adequate model. The proposed circuit model of an AC motor with feeding cable is presented in Fig. 5, where the AC motor is represented as an *N*-rung *LC* ladder circuit whereas the feeding cable is represented as a lossy transmission line. The

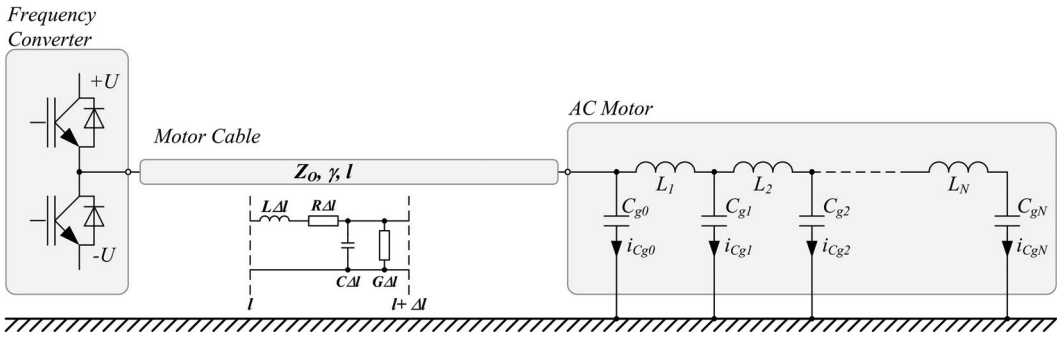

Fig. 5. Circuit model of AC motor winding with feeding cable for broadband CM currents analysis - simplified one phase representation

foremost benefit of using circuit models is its relatively low complexity level in relation to the achieved accuracy. A reasonable balance kept between model simplicity and their adequacies allows for significant reduction of its parameters identification efforts and decrease radically computational overheads of the simulation analysis. An identification of parameters of the circuit model of the AC motor with feeding cable can be completed based on the terminal impedance measurement. Based on this model, various simulations have been carried out using the motor and the feeding cable parameters which are identified experimentally. Examples of simulation results obtained for the tested AC motor an AC motor with the feeding cable are presented in Fig. 6.

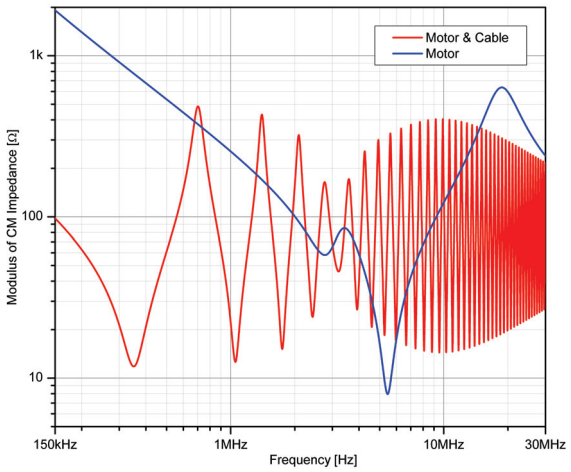

Fig. 6. Example of simulation results of CM impedance of evaluated AC motor and AC motor with feeding cable

Presented simulation results allow investigating the influence of the feeding cable on the CM impedance changes. Particularly, the observed decrease of the frequencies for which the CM impedance of the converter loads approaches lowest values can be successfully analyzed for different feeding cable lengths.

Experimental Verification of the Broadband Model

Experimental investigation of CM current generation and propagation has been done for a typical ASD with voltage source inverter (VSI) feeding AC motor, both of rated power *7.5 kW*. A four pole, *50 Hz* AC motor with no mechanical load was connected to the converter's output terminals by a three wire shielded cable. Two lengths of feeding cables have been used: the first one was very short (less than *0.2 m*) and the second one was relatively long *100 m*). In both cases the cable shield was connected at both ends to the reference ground: one of them to converter ground terminal and the other one to the AC motor grounding terminal.

Configuration of the experimental test bench is presented in Fig. 1 where the AC motor CM currents $I_{CM,M}$ have been measured for both lengths of AC motor feeding cable. The CM current probe has been inserted onto the very short unshielded section of feeding cable, as close as possible to the motor winding terminals. Additionally the input side of the evaluated converter was fed through a line impedance stabilization network (LISN) in order to minimize power grid impedance influence on the obtained measurement results.

Measurement results calculated as a ratio between AC motor CM currents recorded for the motor with short and long feeding cable are presented in Fig. 7. Based on the obtained measurement results, in the evaluated frequency range CISPR (*150kHz-30MHz*), few characteristic frequency sub ranges related to the analyzed feeding cable influence on the AC motor CM currents can be determined. In the frequency range below *2 MHz* an increase of motor CM current was remarked, especially for the frequency ranges closely correlated with the impedance characteristic of feeding cable (*350 kHz*, *1 MHz* and *1.07 MHz*).

The maximum increase, approximately 15 dB, was recorded for frequency of about *350 kHz*. Decrease of the motor CM current, caused by feeding cable, was noticed for the frequencies higher than *2 MHz*. The maximum attenuation effect of feeding cable (about *-20 dB*) in the frequency range about *4-6 MHz* is closely correlated with the AC motor reflection characteristic presented in Fig. 3 and winding CM impedance presented in Fig. 7. For frequency range above 6 MHz the measured CM current attenuation effect of motor feeding cable became lower, correspondingly with motor windings reflection characteristic (Fig. 3).

Simulation result obtained basing on the proposed simplified circuit model are presented in comparison to the experimental results in Fig. 7. Presented comparison shows that the investigated circuit model characterizes accurately frequency ranges in which the AC motor CM currents are noticeably increased due to the feeding cable resonances. Nevertheless, the levels of increase obtained by simulation are noticeably higher in comparison to measurement results. It is a result of numerous simplifications assumed in model development, especially related to dielectric losses in cable and motor winding. The frequency dependence of dielectric losses where not sufficiently represented in the model, therefore the simulation results are overestimated in HF range. In the frequency range above the motor winding main resonance, in the investigated case above $\sim$*4 MHz,* the magnitudes of CM currents obtained by simulation are not adequate enough due to underestimated losses in the model. However, the multi-resonance response of the converter's load in that frequency range is clearly illustrated by the model.

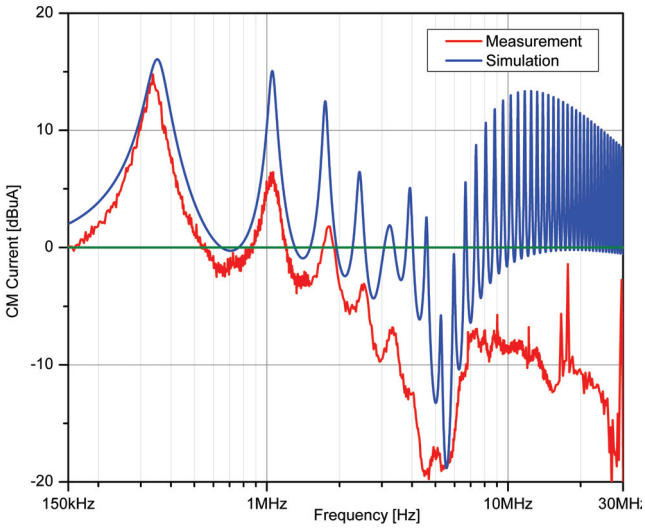

Fig. 7. Measurement and simulation results of the influence of motor feeding cable on the CM current of AC motor

Conclusions

The main objective of the presented work was to investigate the influence of the AC motor feeding cable on the motor CM currents magnitudes. Detailed modeling of high frequency interactions occurring at output side of frequency inverter, motor cable and AC motor windings require broadband model's, which are enormously complex to parameterize, because of many parameters which have to be determined, usually based on experimental measurement. The proposed simplified circuit model of the converter load is relatively in-elaborate and its parameters are rather effortless to determine. Experimental verifications of the simulation results, which have been done for the investigated ASD based on this model, shows that the capability of such model can be sufficient enough for analysis of motor feeding cable influence on the motor CM current. Results of experimental and simulation investigations confirm that motor feeding cable has significant influence on the generation of AC motor CM current, which are essential for EMI emission of ASD. Simplified broadband circuit modeling of converters load allows determining characteristic frequency ranges in which motor cable influence is mostly significant. In the frequency range above the main resonance frequency of motor winding more detailed determination of motor feeding cable influence on CM current emission requires more advanced models. Obtained simulation results are generally overestimated to the experimental, especially above 2 MHz, due to the underestimation of HF dielectric losses in the evaluated model and characterize worst case scenario.

REFERENCES

[1] S. Ogasawara, H. Akagi; Analysis and Reduction of EMI Conducted by a PWM Inverted-Fed AC Motor Drive System Having Long Power Cables, Proc. of IEEE 31st Annual Power Electronics Specialists Conference (PESC'00), Vol. 2, 2000, pp. 928-933.

[2] J. Adabi, F. Zare, G. Ledwich, A. Ghosh; Leakage Current and Common Mode Voltage Issues in Modern AC Drive Systems, AUPEC, Perth, Australia, Dec 2007.

[3] J. Luszcz, K. Iwan; AC motor transients and EMI emission analysis in the ASD by parasitic resonance effects identification, European Conference on Power Electronics and Applications, EPE 2007.

[4] F. Zare; Modeling of Electric Motors for Electromagnetic Compatibility Analysis, AUPEC 2006, Melbourne, Australia, Nov 2006.

[5] A. Said, K. Al-Haddad; A new approach to analyze the overvoltages due to the cable lengths and EMI on adjustable speed drive motors, Power Electronics Specialists Conference, 2004. PESC 04. 2004 IEEE 35th Annual, Volume 5, 20-25 June 2004 Page(s):3964 - 3970 Vol. 5.

[6] T. Weidinger; Elimination of increased excitation of common-mode oscillations in electrical drive systems with active front end and long motor cables, Power Electronics and Motion Control Conference, 2008. EPE-PEMC 2008.

[7] F. Zare; High frequency model of an electric motor based on measurement results Australian Journal of Electrical & Electronics Engineering (AJEEE), Vol 4, No 1, 2008, page 17-24.

[8] L. Arnedo, K. Venkatesan; High frequency modelling of induction motor drives for EMI and overvoltage mitigation studies; Electric Machines and Drives Conference (IEMDC'03), Volume 1, 1-4 June 2003 Page(s): 468 - 474.

[9] J. Luszcz, I. Moson; AC Motor Windings Circuit Model for Common Mode EMI Currents Analysis' The 5th International Conference CPE 2007, Compatibility in Power Electronics, May 29 - June 1, 2007, Gdansk, Poland.

[10] A.F. Moreira, T.A. Lipo, G. Venkataramanan, S. Bernet; High-frequency modelling for cable and induction motor over voltage studies in long cable drives, IEEE Transaction on Industry Application vol.38, no.5, pp.1297–1306, 2002.

[11] N. Hanigovszki, J. Poulsen, G. Spiazzi, F. Blaabjerg; An EMC evaluation of the use of unshielded motor cables in AC adjustable speed drive applications", Power Electronics Specialists Conference, 2004. PESC'2004. Volume 1, 20-25 June 2004 Page(s):75 - 81 Vol.1.

[12] J.Luszcz; Motor Cable as an Origin of Supplementary Conducted EMI Emission of ASD', 13th European Conference on Power Electronics and Applications (EPE 2009), 8 - 10 September 2009, Barcelona, Spain.

[13] J.Luszcz; Motor Cable Influence on the Converter Fed AC Motor Drive Conducted EMI Emission, The 5th International Conference CPE 2009, Compatibility and Power Electronics, May 20 - 22, 2009, Badajoz, Spain.

[14] A. Muetze, A. Binder; Calculation of Circulating Bearing Currents in Machines of Inverter-Based Drive Systems, IEEE Transactions on Industrial Electronics, Volume 54, Issue 2, April 2007 Pages:932 – 938.

[15] H. Akagi, S. Tamura; A passive EMI ?lter for elimination both bearing current and ground leakage current from an inverter-driven motor, IEEE Trans. Power Electronics, vol. 21, no. 5, pp. 1459–1469, Sep. 2006.

[16] J. Adabi, F. Zare, A. Ghosh; End-winding Effect on Shaft Voltage in AC Generators, 13th European Conference on Power Electronics and Applications (EPE 2009), 8 - 10 September 2009, Barcelona, Spain.

[17] A. Kempski, R. Strzelecki, R. Smolenski, Z. Fedyczak; Bearing current path and pulse rate in PWM-inverter-fed induction motor, PESC. 2001 IEEE, Volume: 4 , 17-21 June 2001 Pages:2025 - 2030 vol. 4.

[18] G. Costabile, B. Vivo, L. Egiziano, V. Tucci, M. Vitelli, L. Beneduce, S. Iovieno, A. Masucci; An accurate evaluation of electric discharge machining bearings currents in inverter-driven induction motors, European Conference on Power Electronics and Applications (EPE 2007) 2-5 Sept. 2007.

[19] A. Muetze, A. Binder; Calculation of motor capacitances for prediction of discharge bearing currents in machines of inverter-based drive systems, 2005 IEEE International Conference on Electric Machines and Drives, Page(s): 264 – 270.

[20] N. Hanigovszki, J. Landkildehus, G. Spiazzi, F. Blaabjerg; An EMC evaluation of the use of unshielded motor cables in AC adjustable speed drive applications, IEEE Transactions on Power Electronics, Volume: 21 , Issue: 1, 2006 , Page(s): 273 - 281.

[21] C.R. Paul: Introduction to Electromagnetic Compatibility, New York: John Wiley & Sons, 1992.

[22] J. Luszcz: Motor cable effect on the converter fed AC motor common mode current, Compatibility and Power Electronics (CPE), 2011 7th International Conference-Workshop Page(s): 445 - 450.

Authors: Jaroslaw Luszcz, Ph.D.,
Gdansk University of Technology, Faculty of Electrical and Control Engineering, Sobieskiego 7, 80-216 Gdansk, Poland, email: jlusz@ely.pg.gda.pl